JOURNAL OF BACTERIOLOGY, July 1992, p. 4463–4474
0021-9193/92/134463-12$02.00/0

Vol. 174, No. 13

Heat Killing of Bacterial Spores Analyzed by Differential Scanning Calorimetry

BRIAN H. BELLIVEAU, TEOFILA C. BEAMAN, H. STUART PANKRATZ, AND PHILIPP GERHARDT*

Department of Microbiology, Michigan State University, East Lansing, Michigan 48824-1101

Received 25 November 1991/Accepted 28 April 1992

Thermograms of the exosporium-lacking dormant spores of *Bacillus megaterium* ATCC 33729, obtained by differential scanning calorimetry, showed three major irreversible endothermic transitions with peaks at 56, 100, and 114°C and a major irreversible exothermic transition with a peak at 119°C. The 114°C transition was identified with coat proteins, and the 56°C transition was identified with heat inactivation. Thermograms of the germinated spores and vegetative cells were much alike, including an endothermic transition attributable to DNA. The ascending part of the main endothermic 100°C transition in the dormant-spore thermograms corresponded to a first-order reaction and was correlated with spore death; i.e., >99.9% of the spores were killed when the transition peak was reached. The maximum death rate of the dormant spores during calorimetry, calculated from separately measured *D* and *z* values, occurred at temperatures above the 73°C onset of thermal denaturation and was equivalent to the maximum inactivation rate calculated for the critical target. Most of the spore killing occurred before the release of most of the dipicolinic acid and other intraprotoplast materials. The exothermic 119°C transition was a consequence of the endothermic 100°C transition and probably represented the aggregation of intraprotoplast spore components. Taken together with prior evidence, the results suggest that a crucial protein is the rate-limiting primary target in the heat killing of dormant bacterial spores.

How do bacterial spores resist heat, and, conversely, how are they killed when their thermal-defense mechanisms are overcome? Answering these two questions is fundamentally important to practical solutions of food spoilage, food poisoning, and infectious disease in which spores are causative. Furthermore, much of microbiological practice depends on heat sterilization, which is predicated on killing all spores in the material.

The question of heat resistance mechanisms now seems mainly answered as follows: bacterial spores are able to resist heat because their protoplasts have become dehydrated to a water content that is low enough to immobilize and therefore to protect the vital macromolecules (e.g., proteins, RNA, and DNA) from denaturation and the supramolecular assemblies (e.g., membranes and ribosomes) from disruption. Although dehydration is the only property necessary and sufficient in itself to impart heat resistance, it is enhanced by mineralization (especially by calcification) and thermal adaptation. The physiological processes by which the spore attains the resistant state are less well understood, but the retention of resistance clearly is a function of an intact peptidoglycan cortex encasing the protoplast. The experimental evidence supporting these assertions has been reviewed by Gerhardt and Marquis (19).

The question of heat killing mechanisms, however, remains mainly unanswered. In an effort to obtain experimental evidence about these mechanisms, we undertook the study of a selected spore morphotype, *Bacillus megaterium* ATCC 33729, which lacks the superficial exosporium layer and can be chemically divested of the coat and outer membrane, leaving only the structures essential to heat resistance, i.e., the cortex-encased protoplast (23). Heat inactivation of the spores was analyzed by use of a computer-controlled differential scanning calorimeter. Differential scanning calorimetry (DSC) is a thermal-analysis technique that has become a powerful tool for detecting and quantifying thermotropic transitions of various materials (10, 13). The DSC method is usually used to characterize isolated biopolymers and macromolecular assemblies but has also been applied successfully to characterize more complex systems such as mammalian cells (24, 25, 27), bacterial vegetative cells (2, 9, 26, 30, 31, 37, 46), and bacterial spores (32–34, 37). DSC can be used to determine the enthalpy of a thermally induced transition by measuring the differential heat flow required to maintain a sample and an inert reference at the same temperature. DSC measures the excess specific heat (i.e., the heat absorbed or lost) in a continuous manner as a function of increasing temperature at a fixed scan rate. When a multicomponent object like a cell is heated, there occurs a sequence of transitional events which cause small perturbations to the specific heat capacity of the cell. These perturbations can be sensed by DSC and recorded as a characteristic pattern of positive transitions (endotherms) and negative transitions (exotherms) representing various cellular components. DSC profiles are analogous to low-resolution gel electrophoresis profiles, except that the separation of DSC peaks is determined by thermostability rather than by mass or charge (25).

Our results with DSC showed that only a few defined transitions are obtained with dormant spores. We were able to identify each of the transitions and correlate the largest irreversible endothermic transition with spore killing. We also compared the heat-induced release of dipicolinic acid (DPA) with spore killing, finding that most of the DPA was released after most of the spores were killed. Taken together with previous DSC and kinetic evidence (see Discussion),

* Corresponding author.

our results suggested that a crucial protein is the rate-limiting primary target in the heat killing of dormant spores.

MATERIALS AND METHODS

Dormant native spores. The spores of *B. megaterium* ATCC 33729 were selected for study primarily because they lack an exosporium and can readily be chemically divested of their coat-outer membrane complex. Neither layer is essential for the maintenance of spore heat resistance and dormancy (23). Thus, this morphotype strain enabled the identification of thermal transition events in the essential cortex-encased protoplast (sporoplast) of the spore. When first isolated, this strain was thought to be an exosporium-lacking variant of *B. megaterium* QM-B1551, ATCC 12872 (23). Later, however, we found that strain 33729 contains two plasmids, whereas strain QM-B1551 contains seven plasmids; therefore, the two strains are unlikely to be directly related.

The dormant native spores were produced in 2-liter Erlenmeyer flasks containing 400 ml of supplemented nutrient broth (43), which were inoculated (5% [vol/vol]) with a 6-h culture and aerated on an orbital shaker (150 rpm) at 30°C for 24 h. Each spore crop was washed repeatedly with sterile deionized water, with low-speed centrifugation (1,500 × *g*) to prevent pressure germination, to 99.9% purity of brightly refractile dormant spores.

Dormant decoated spores. The dormant native lysozyme-resistant spores were divested of their coat-outer membrane complexes and thus were converted to lysozyme-susceptible, decoated, but still dormant spores by treatment at pH 10 with 0.5% sodium dodecyl sulfate (SDS), 0.1 M dithiothreitol, and 0.1 M NaCl (16, 44). They were purified as described above for dormant native spores.

Cortex sacculi. Intact cortical murein (peptidoglycan) sacculi were isolated by a modified Park-Hancock fractionation (41) as described by Marquis and Bender (36). The decoated spores were successively extracted with cold (0°C) 5% trichloroacetic acid, 70% ethanol, hot (90°C) 5% trichloroacetic acid, and boiling 3% SDS. The resulting cortex sacculi retained both the ellipsoidal shape and the refractility of the spores, but with the remaining cytoplasm denatured and congealed.

Activated native spores. The dormant native spores were activated by heating them in a water bath for 20 min at 65°C.

Germinated native spores. Since there are no known chemical germinants for the spores of this strain (23), the activated native spores were pressure germinated by first centrifuging them at 5,000 × *g* and then allowing the resulting compact pellet to stand overnight at 4°C, after which 95% of the spores had become spherical and phase-dark.

Vegetative cells. Vegetative cells were either grown from spore inoculum on tryptic soy agar (Difco) at 30°C for 24 h, for comparison with the results of Miles et al. (37) by this procedure, or harvested at 6 h from the broth culture described above for dormant native spores.

Heat resistance. The resistance of the spores to moist heat was determined at 70, 80, 85, and 90°C and expressed as a *D* value (the number of minutes required for a 10-fold reduction in the number of CFU), as described previously (5). The *D* values were then plotted versus temperatures to generate *z* values (the temperature change needed to reduce the *D* values by a factor of 10).

Calorimetry. Spore and vegetative-cell samples for DSC analysis were taken from dense aqueous suspensions. A sample (equivalent to 10 to 15 mg [dry weight] for spores and 7 to 10 mg [dry weight] for vegetative cells) was crimp sealed in a 70-μl gasketed stainless steel pan, which was first cooled to 10°C and then heated in the differential scanning calorimeter (model DSC-7; Perkin-Elmer Corp., Norwalk, Conn.) at a rate of 10°C/min from 10 to 135°C, with an empty, sealed pan used as the reference. Partial scans to lower temperatures were sometimes made. Afterward, the pans were rapidly cooled (200°C/min) to the initial temperature and then immediately rescanned to determine the reversibility of the transitions in the initial scan. The amounts of sample dry weight were determined by either piercing the pan after or removing a subsample before the DSC analysis and drying in an oven at 90°C under vacuum for 18 h. The temperature scale of the calorimeter was calibrated according to the manufacturer's instructions with the melting points of indium and zinc as standards.

Since the linearity of the baseline was checked regularly, the scans did not require correction for baseline curvature. All of the scans shown represent at least three separate experiments. The heat flow in milliwatts recorded by the calorimeter was converted to relative excess specific heat (C_p) expressed as Joules per kilogram per degree Celsius. Positive deflections of C_p represent the heat absorbed due to endothermic processes, and negative deflections represent the heat released due to exothermic processes. The original data profiles from the calorimeter were computer plotted. These profiles were then computer copied and replotted to remove inconsequential irregularities ("noise"), while retaining all experimental irregularities.

Release of DPA and A_{240} to A_{280} materials. Temperature-induced release of DPA from the spores was monitored by heating a series of sample pans to successively higher temperatures within a transition. After being heated to a given temperature, each pan was cooled to its initial temperature and removed from the calorimeter. Each pan lid was carefully removed, and each spore sample was suspended in 5 ml of distilled water. The spore suspension was centrifuged at 5,000 × *g* for 10 min at 4°C, and the supernatant fluid was removed. DPA in the supernatant fluid was then assayed as described by Janssen et al. (20) and expressed as micromoles of DPA per spore. There resulted a scan of DPA release versus temperature, directly comparable to the heat capacity scan.

The supernatant fluid was also examined for the release of cytoplasmic material (DPA, proteins, and nucleic acids) absorbing between 240 and 280 nm, with a Beckman model DU-50 spectrophotometer.

Electron microscopy. The methods for electron microscopy were essentially those described previously (3, 4). Fixed, embedded spores were cut into thin sections and then stained with uranyl acetate and lead citrate. Transmission micrographs were obtained with a Philips model CM-10 electron microscope.

Calculations. The calculations of various thermal parameters were made by use of the equations derived by Bigelow (6) and Rahn (42), as modified by Miles et al. (37), as follows. The mathematical designations for natural exponential functions used by Miles et al. are retained here for clarity in the more complex equations. That is, $\exp(x) = e^x = 2.303^x$.

The thermal inactivation of spores, at a constant temperature, is generally considered to be a pseudo-first-order process, expressed by the equation $N = N_o \exp(-kt)$, where N is the number of surviving spores after a heat treatment of t minutes in a suspension initially containing N_o spores and

where k is the specific death-rate constant. From the definition of D (see the section above on heat resistance), $k = \frac{2.303}{D}$.

An equation that relates D to the value A at any arbitrary temperature T and to the value D_e at a particular temperature T_e is as follows:

$$D = D_e \exp\left(\frac{T_e - T}{A}\right) \quad (1)$$

where $A = \frac{z}{2.303}$ and where z is as defined in the section above on heat resistance.

If the temperature of the sample is increased from the starting temperature T_o at a constant scan rate r, the temperature at any instant in time t is given by the equation $T = T_o + rt$.

The number of surviving spores N_o at any temperature can then be obtained from the following equation:

$$\frac{N}{N_o} = \exp\left\{\frac{-z}{D_e r}\left[\exp\left(\frac{T - T_e}{A}\right) - \exp\left(\frac{T_o - T_e}{A}\right)\right]\right\} \quad (2)$$

The rate at which the population is inactivated per unit of time can also be expressed by the following equation:

$$\frac{l}{N_o}\frac{dN}{dt} = \frac{-2.303}{D_e}\exp\left(\frac{T - T_e}{A}\right) \exp\left\{\frac{-z}{D_e r}\left[\exp\left(\frac{T - T_e}{A}\right) - \exp\left(\frac{T_o - T_e}{A}\right)\right]\right\} \quad (3)$$

The rate at which the population is inactivated per unit of increase in temperature can be calculated from equation 3 by the following relationship:

$$\frac{1}{N_o}\frac{dN}{dT} = \frac{1}{rN_0}\frac{dN}{dt} \quad (4)$$

Equation 4 essentially describes the predicted DSC profile for spore inactivation as well as the predicted profile for irreversible denaturation of the critical target if the temperature dependence for denaturation of the critical target is assumed to be the same as the temperature dependence for spore inactivation.

The temperature $T_{D_{max}}$, where the inactivation rate is maximum, is then obtained by differentiating the logarithm of equation 3 and setting it equal to zero thus:

$$T_{D_{max}} = T_e + \frac{z}{2.303}\ln\left(\frac{D_e r}{z}\right) \quad (5)$$

The temperature width at half the peak height (ΔT) describes the width of the predicted DSC peak generated from equation 5, giving the following equation:

$$\Delta T = 1.062z \quad (6)$$

A somewhat similar mathematical approach for describing cell killing in a calorimeter was published by Lepock et al. (27), except that their equations were derived from the Arrhenius relationship.

RESULTS

Dormant native spores. DSC thermograms (scan profiles of the relative excess specific heat values versus temperature values) were obtained first for dormant native spores of *B. megaterium* ATCC 33729, as shown in Fig. 1A. Their appearance in electron micrographs of stained thin sections is depicted in Fig. 2A. Their initial-scan profile showed three major endothermic transitions with peaks at 56, 100, and 114°C (identified as *a*, *b*, and *c*, respectively) and a major exothermic transition with a peak at 119°C (identified as *d*). No further transitions were observed when these and other scans were extended beyond the 135°C terminus, e.g., to 200°C (data not shown). The rescan profile of the spores showed no transitions, indicating that all of the initial-scan transitions were not reversible. The term transition refers to the sequence of molecular events responsible for each peak. The transition temperature (T_m) refers to the temperature at maximum or minimum C_p for each peak, as listed in Table 1.

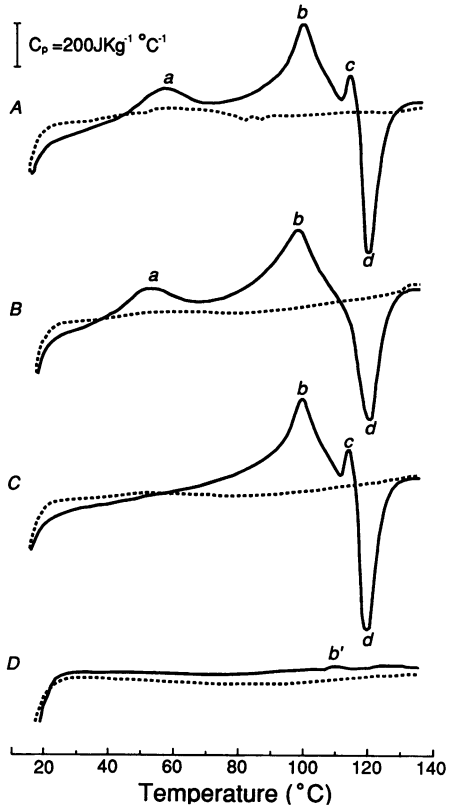

FIG. 1. DSC profiles of dormant native spores (A), dormant decoated spores (B), activated native spores (C), and cortex sacculi (D), all of *B. megaterium* ATCC 33729. The major thermal transitions are identified at their peaks as *a*, *b*, *c*, and *d*. Endothermic transitions are positive (upward peaks), and exothermic transitions are negative (downward peaks). The solid lines are the initial scans. The broken lines are the rescans that were made after the samples were cooled to the starting temperature, demonstrating the irreversibility of the transitions. A minor reversible transition on the rescan of the cortex sacculi is identified at its peak as *b'*.

It was not possible to assign specific cellular components to each transition, but most of the enthalpic heat absorbed must be due to protein denaturation with contributions possibly from DNA and RNA unfolding, from alterations (especially depolymerization) of complex cellular structures, and from denaturation-induced aggregation of macromolecules (27). Transitions involving such denaturation, unfolding, or melting reactions are endothermic. Depolymerization and aggregation reactions are more complex and may be either endothermic or exothermic. Presumably, contribu-

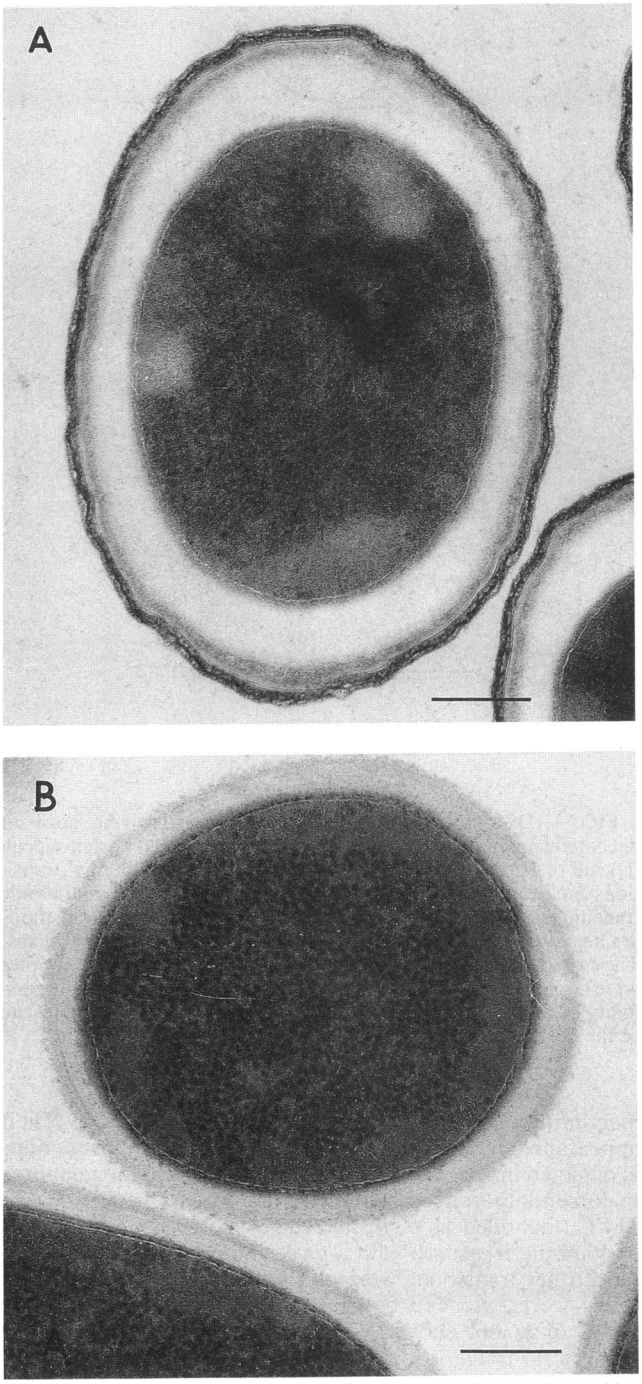

FIG. 2. Electron micrographs of representative stained thin-sectioned spores. (A) Dormant native spore with peripheral coat and underlying outer membrane; (B) dormant decoated spore with peripheral cortex and underlying protoplast.

tions in enthalpy from both depolymerization and aggregation should be small, i.e., probably less than 1% of the total enthalpy of all transitions measured for the spores. The difference seen between the initial-scan profile and the rescan profile was attributable to cellular components undergoing irreversible transitions. Therefore, by subtracting the rescan from the initial scan to obtain a difference scan, the contributions from membrane lipids and that portion of DNA and RNA that can renature should be removed. Since all of the transitions observed for dormant native spores were irreversible, including those of DNA and RNA, no useful information was obtained from the difference scans with regard to the enthalpic contributions of these usually reversible transitions (data not shown).

The DSC thermogram of a spore is complex in that it represents the sum of all cellular transitions, and there may be thousands of potential endothermic transitions in a heated spore due to the processes mentioned above. Thus, each major transition in a scan may represent a composite of many minor transitions, a transition in a component that is present in high concentration, a cooperative transition of strongly interacting components, or a set of coupled transitions. The profiles are such that the individual transitions of each cellular component are not resolvable. Minor processes in terms of ΔC_p, e.g., the breaking of covalent bonds in a few copies of a critical macromolecule, may be critical for spore killing but not detectable by DSC.

The area under a DSC thermogram represents the total enthalpy of all component transitions. The total enthalpy of the dormant native spore, obtained from the onset of transition *a* (40°C) to the end of transition *c* (116°C) (Fig. 1A), was 25.9 J per g (dry weight). The rescan showed that the heat-killed spores had a slightly higher specific heat capacity at lower temperatures than did the viable spores in the initial scan. This is usual, as was noted by Miles et al. (37) for vegetative bacterial cells, because there normally is an increase in specific heat upon going from the native to the denatured state.

Dormant native spores of *B. megaterium* QM-B1551 (for electron micrograph, see Fig. 1 in reference 23) were also scanned to determine whether its outermost exosporium layer, common to many spore species but not to strain ATCC 33729, would contribute to the DSC profile of spores. The DSC scans of QM-B1551 spores revealed no distinct transition attributable to the exosporium (data not presented), which is consistent with results shown by Maeda et al. (32) for the exosporium-containing spores of *Bacillus cereus*. The numbers and positions of the observed transitions were similar to those of the ATCC 33729 scans (Fig. 1A), except that the magnitude of transition *d* was smaller and the magnitude of transition *c* was greater in the QM-B1551 spores. These spores were difficult to prepare for DSC analysis in that they did not form the necessary compact pellet upon centrifugation.

Dormant decoated spores. Next, an effort was made to identify the sporal component(s) or physiological state(s) associated with each major peak in the DSC thermogram of the dormant native spores of strain ATCC 33729. Figure 1B shows the thermogram obtained with the spores after treatment with SDS and dithiothreitol to remove the coat and outer membrane. The electron micrograph in Fig. 2B shows that the peripheral coat-outer membrane layer of the native spore was completely divested, leaving a stable cortex-encased protoplast that still retained spore-characteristic heat resistance (Table 1).

The thermogram difference between the native and decoated spores should be attributable to the coat and outer membrane, and this was shown by the loss of transition *c*. This transition probably represented the composite transition of the coat proteins. A transition of the outer membrane component of the coat complex would likely have occurred with a peak at about 20°C, the expected temperature for melting of membrane lipids (26, 45), and therefore would not likely have contributed to transition *c*.

The peak temperatures of transitions *a* and *b* shifted from 56 to 53°C and from 100 to 98.5°C, respectively, in the

TABLE 1. Numerical description of DSC scans and calculated inactivation rate characteristics of various cell types of *B. megaterium* ATCC 33729[a]

Cell type	T_e (°C)	D_e (min)	z (°C)	$T_{D_{max}}$ (°C)	ΔT (°C)	T_o (°C)	Temperature at peak of transition, T_m (°C)									
							a	*b*	*b'*	*c*	*d*	*e*	*f*	*g*	*g'*	*h*
Dormant native spores	70	4,651	6.2	94.5	6.6	73.5	56.2	100		114	119					
	80	140														
	90	3.3														
	100	0.045														
Dormant decoated spores	70	1,277	6.2	91.0	6.6	68.0	53.0	98.5		114	119					
	80	85.5														
	90	0.91														
	100	0.033														
Activated native spores								100		114	119					
Cortex sacculi									110							
Germinated native spores	47	7.0				47.3						72.3	82.5	97.3		120
Vegetative cells	47	5.0				45.0						72.3	82.5	91.0	91.0	107

[a] T_e is the temperature at which D_e was determined. D_e and z values are from Koshikawa et al. (23). $T_{D_{max}}$ is the temperature at which a critical target inactivation transition was at maximum (i.e., at its peak), as shown in Fig. 8. ΔT is the half-width of a critical target inactivation transition at half its maximum height. T_o is the onset of thermal denaturation. *a*, *b*, *b'*, *c*, and *d* are the transitions identified in Fig. 1. *e*, *f*, *g*, *g'*, and *h* are the transitions identified in Fig. 2.

decoated spores (Fig. 1B). This was accompanied by a corresponding reduction in heat resistance of the decoated spores (Table 1), suggesting that a correlation may exist between sporal heat resistance and the peak temperatures of transitions *a* and *b*. This further implies that transition *a* is somehow linked to heat resistance, even though its temperature span occurs below lethal temperatures for this spore.

Activated native spores. Sublethal heat (heat shock) is known to activate dormant *B. megaterium* spores, increasing both the rate and extent of germination (28). As shown in Fig. 1C, transition *a* was absent when the spores were scanned immediately after being activated in the usual way (i.e., heated at 65°C for 20 min in a water bath and then cooled in an ice bath). Furthermore (see Fig. 6B and B'), transition *a* disappeared when the spores were scanned to 65°C, cooled, and then rescanned. However, transition *a* reappeared in the scan after heat-activated spores were stored at 4°C for 6 weeks (data not shown), confirming the reversibility of the process after lengthy incubation (11, 22, 34). Since denaturation of the macromolecule(s) related to maintenance of spore dormancy or inactivation of the component that prevents spore germination is probably the main step in activation (21, 22, 34), it seems likely that transition *a* represents the denaturation or conformational change of protoplast macromolecules leading to the heat-activated state (17, 29).

The spores that had been heat activated by scanning to 65°C were tested for their ability to germinate in nutrient broth. Their loss of refractility, detected by phase microscopy and by an 85% decrease in optical density at 600 nm after 60 min of incubation, confirmed that these spores were indeed heat activated and germinable (data not shown).

No apparent morphological differences in fine structure were observed between the dormant native spores (Fig. 2A) and activated native spores (data not shown), unlike the difference observed in the spores of *Bacillus anthracis* (38) and *Bacillus stearothermophilus* (4).

Cortex sacculi. In order to determine whether the cortical peptidoglycan layer of the dormant spore contributed to any of the transitions observed with the dormant native spores, intact cortex sacculi (Fig. 3) were isolated from the dormant spores and examined by DSC (Fig. 1D). There was detected a very minor irreversible endothermic transition with a peak at 110°C (identified as *b'*), and this transition was resolved more clearly when the C_p scale was amplified threefold (data not shown). This transition was not observed in the scans of native, decoated, and activated spores probably because it was masked by transitions *b* and *c* in each of these different spore types. Regardless, the contribution to the total specific heat capacity of the spore by the cortex was negligible.

Germinated native spores. Native spores that had been heat activated and then pressure germinated produced DSC thermograms that were markedly different from those of the dormant and activated spores. The profile for germinated native spores (Fig. 4A) showed four major endothermic

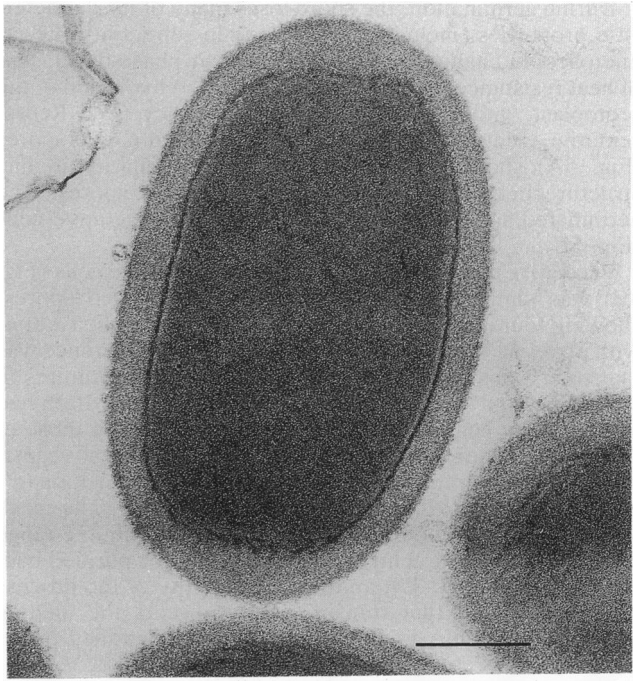

FIG. 3. Electron micrograph of a representative stained thin-sectioned cortex sacculus. Note the homogeneous appearance of its denatured congealed cytoplasm, in contrast to the differentiated appearance of the cytoplasm in the native spores (Fig. 2).

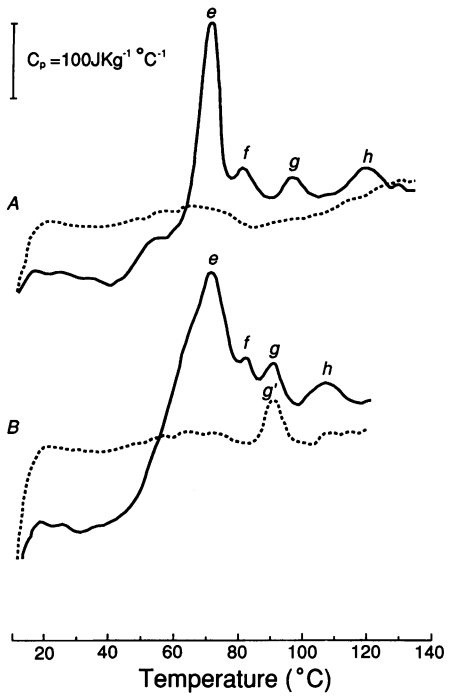

FIG. 4. DSC profiles of germinated native spores (A) and vegetative cells (B). The major thermal transitions on the initial scans are identified at their peaks as *e*, *f*, *g*, and *h*. A major reversible transition on the rescan of the vegetative cells is identified at its peak as *g'*.

transitions (*e* to *h*), with peaks at 72, 83, 97, and 120°C. There were no exotherms. All four transitions were irreversible, as shown by their disappearance in the rescan.

During germination, the spore loses many of its characteristic properties, including a decrease in refractility (i.e., a microscopic change from phase-bright to phase-dark), loss of heat resistance, increase in stainability, rehydration of the protoplast, and breaking of spore dormancy (17). Representative electron micrographs of germinated native spores (Fig. 5A) showed that there was little similarity in fine structure between them and dormant native spores. The germinated spores more closely resembled vegetative cells (Fig. 5B).

Vegetative cells. The DSC profile for vegetative cells (Fig. 4B) was similar to that obtained for germinated spores, showing four major endothermic transitions (labelled *e* to *h*) with peaks at 72, 83, 91, and 107°C. The main difference was that transitions *g* and *h* occurred at higher temperatures in the germinated spores than in the vegetative cells. Both had similarly low heat resistance levels compared with those of the dormant spores (Table 1). In the DSC rescan of vegetative cells, there remained a major endothermic transition (*g'*) with a peak at 91°C, indicating reversibility. The peak temperature of *g* and *g'* (both at 91°C) was within the range of midpoint melting temperatures reported for purified bacterial DNA (12, 35, 37), and the reversibility of the process further indicated that transition *g* represents the melting endotherm of DNA in vegetative cells, as identified previously by Miles et al. (37).

The peak temperature of transition *g* was about 6°C higher in germinated spores than in vegetative cells and was irreversible. This suggested that, under the physiological conditions within the germinated spore, the thermostability

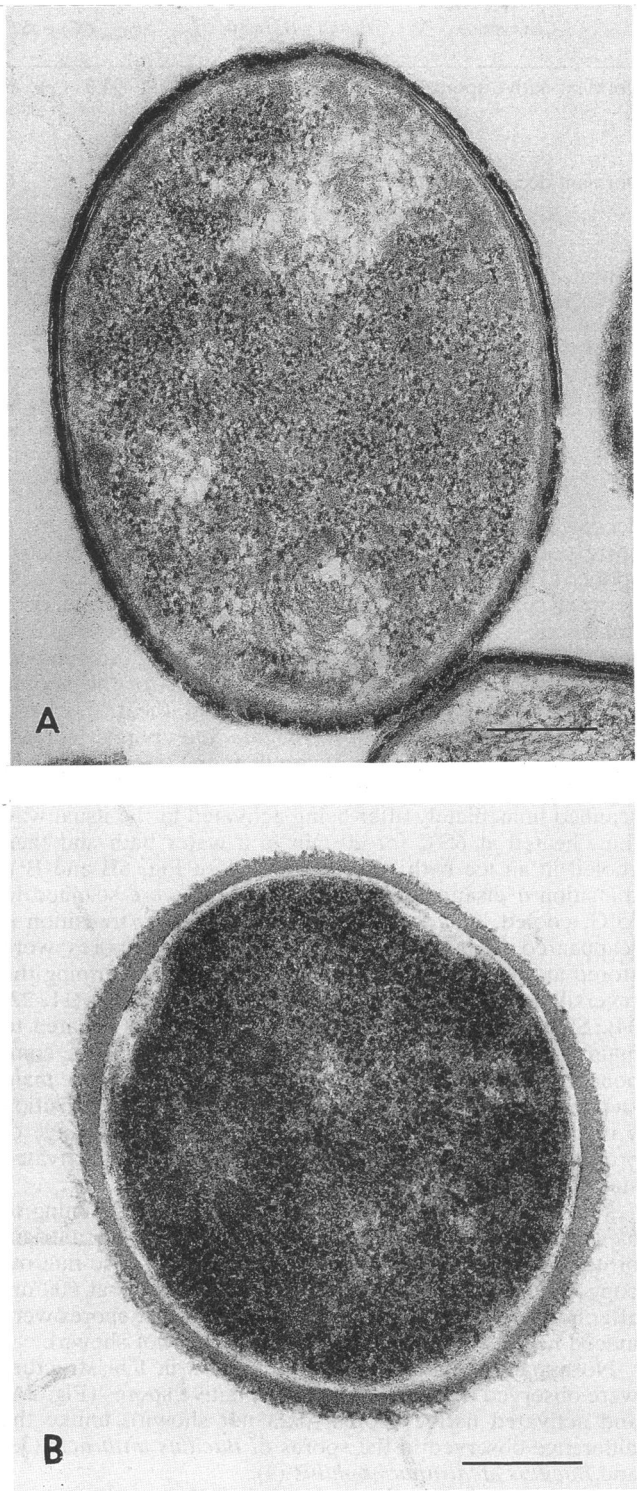

FIG. 5. Electron micrographs of a representative germinated native spore (A) and a vegetative cell (B). Note the resemblance of the cytoplasm of the germinated spore to that of the vegetative cell, rather than to that of the dormant spore.

of DNA was increased and its renaturation was hindered. The germinated spores were slightly more heat resistant than the vegetative cells and therefore might possess some of the sporal properties which would interfere with the denaturation and renaturation kinetics of DNA, e.g., incomplete rehydration of the protoplast.

The much greater thermostability of dormant spores, in general, is due to the fact that the protoplast of the dormant spore exists as a dehydrated, closely packed mass of small molecules, ribosomes, DNA, and proteins, all having restricted molecular movement (19). This immobilization of macromolecules may explain why the melting endotherms of DNA seen in vegetative cells and germinated spores were not detectable in the DSC scans of dormant native, dormant decoated, and activated native spores.

Onset temperature of heat inactivation. The onset temperatures of thermal inactivation (T_o) of the different spore types and vegetative cells were determined directly from their DSC scans. This method is much easier and quicker than using conventional killing curves and gives similar values for T_o. For germinated spores and vegetative cells, T_o is best identified as the temperature at which the rectilinear, ascending side of transition *e* (Fig. 4) intersects a horizontal line drawn through the lowest part of the curve (26). The T_o of vegetative cells (45°C) and the T_o of germinated spores (47°C) were both higher than the maximum growth temperature (44°C). Transition *e* was apparently associated with heat killing of the vegetative cells and germinated spores because of its similarity to a major DSC transition that was observed and directly correlated with measurement of cell death in another bacterium (2). Thermal inactivation of the vegetative cells and germinated spores during transition *e* was also indicated by its irreversibility on the DSC rescans (Fig. 4).

For dormant spores, the method for determining T_o was more complicated and less reliable than that for germinated spores and vegetative cells. For example, since transition *a* (Fig. 1A) is correlated with the process of heat activation and since heat activation occurs at sublethal temperatures, then T_o should be higher than the temperature at the end of transition *a*; i.e., $T_o > 65$°C. Furthermore, since spores of this strain can be heat inactivated, albeit slowly, at temperatures as low as 70°C (Table 1), then T_o must be $\geq$70°C. Consequently, the T_o of dormant spores was defined as the temperature of first detectable deviation from a horizontal line drawn through the lowest part of the curve between transitions *a* and *b*. Thus, the T_o of dormant native spores was determined to be 73.5°C and that of dormant decoated spores was determined to be 68°C. Unfortunately, the T_o of activated spores could not be determined directly from the DSC scan.

Altogether, the results indicated that the onset temperature of heat inactivation correlates well with the different heat-resistant states; i.e., the following relationships hold: the T_o and the thermal resistance of dormant native spores > those of dormant decoated spores >> those of germinated native spores > those of vegetative cells (Table 1).

Identification of the inactivation transitions. The identity of transitions *b* and *d* in the DSC thermogram of dormant native spores (Fig. 1A) was sought by taking advantage of the irreversibility of these transitions. A series of partial DSC scans was made sequentially, and then each was rescanned to identify the stable, nondenatured components and the labile, denatured components. This strategy, the results of which are shown in Fig. 6, is similar to that developed previously (26, 34, 47). Figure 6A shows the same thermogram as that in Fig. 1A for dormant native spores but is included here for direct comparisons.

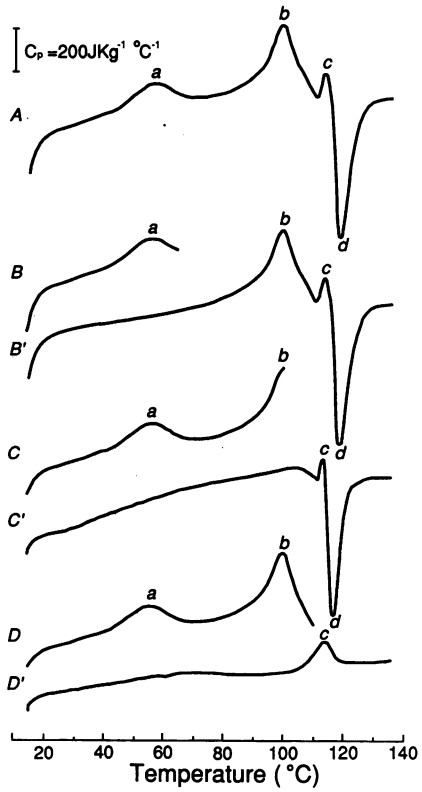

FIG. 6. DSC partial scans and full rescans of dormant native spores. (A) Full reference scan, the same as that shown in Fig. 1A; (B) partial scan to 65°C; (B') full rescan after cooling; (C) partial scan to 100°C; (C') full rescan after cooling; (D) partial scan to 110°C; (D') full rescan after cooling.

Figure 6B shows the results of a partial scan in which the heating was stopped at 65°C near the end of transition *a*. When this sample was cooled and rescanned through the entire temperature range (Fig. 6B'), only transitions *b*, *c*, and *d* remained, each with a magnitude and T_m comparable to those seen in the sample which had not been partially heated (Fig. 6A). The disappearance of transition *a* indicated that it was related to the heat activation process of dormant spores (see section above on activated native spores).

Figure 6C shows the results of a partial scan stopped at 100°C, the peak temperature of transition *b*. When this sample was cooled and rescanned through the entire temperature range (Fig. 6C'), only transitions *c* and *d* remained.

When a spore sample was partially scanned to 108°C at a point near the end of transition *b* (Fig. 6D) and then cooled and rescanned through the entire temperature range (Fig. 6D'), only transition *c* remained (representing the spore coat; see section above on dormant decoated spores), but with a magnitude and area greater than those seen in a sample that had not been partially heated. Thus, in full scans of samples that had not been partially heated (e.g., Fig. 6A), transition *c* seemed smaller than its actual size (e.g., Fig. 6D') because of partial superimposition on either side by transitions *b* and *d*. The persistence of transition *c* after the spores were heated to 108°C indicated that the spore coat retains its native structure beyond the temperature that is lethal for the spore.

The disappearance of exothermic transition *d* in Fig. 6D' indicates that transition *d* was a consequence of endothermic transition *b*. Transition *d* most likely represented the aggregation or coagulation of denatured macromolecular constituents represented by transition *b*. A similar exotherm following a denaturation endotherm has been observed in DSC scans of intact human erythrocytes and attributed to the aggregation of hemoglobin (24).

Isothermal inactivation. To demonstrate that the macromolecular denaturation and aggregation transitions represented by *b* and *d*, respectively, in Fig. 6A and 1A were correlated with killing of the spores, a dormant spore sample was exposed to a constant temperature (set below the peak temperature of transition *b*) until all of the spores had been killed. To achieve this, dormant native spores were held at 90°C for 45 min in the calorimeter. Assuming a D_{90} of 3.3 min (Table 1) and a starting population of approximately 10^{10} spores per ml, all spores in the population would have been killed by 33 min. However, the longer exposure period was used to ensure that even a subpopulation of highly heat-resistant spores would be killed. When the heated sample was cooled and rescanned through the entire temperature range, transitions *b* and *d* were both absent from the thermogram (data not shown). This indicated that, when lethal damage in a spore accumulates for a long period of time at a low temperature, just as much macromolecular denaturation and aggregation can occur as at a high temperature for a shorter period of time (e.g., Fig. 6D').

Critical target analysis. If heat killing of dormant spores is due to the denaturation of a crucial macromolecular component, probably a protein, then the shape and location of the DSC transition of the critical (rate-limiting) target can be predicted. According to target theory, the rate constant for killing (*k*) obtained from the main rectilinear part of a semilogarithmic survivor curve is identical to the rate constant for denaturation of the critical target (15). Accordingly, the amount of spore killing is directly proportional to the extent of denaturation of the target. Measuring the rate of spore killing as a function of temperature thus gives sufficient information to predict the shape of the temperature-induced transition of the critical target.

However, potential complications arise when deviations from exponential death are observed in the survivor curve (1, 8). These include curves with a shoulder followed by exponential death, curves with exponential death initially but followed by a decreasing death rate ("tailing"), sigmoid curves with both a shoulder and tailing, and biphasic rectilinear curves. These types of deviations have been attributed to the presence of two or more discrete populations of differing resistances, to the acquisition of heat resistance during the initial portion of the heating period, to a high degree of clumping, to the requirement for heat activation of spores, to multiple targets, to multiple copies of a single critical target, to repair or replacement of damaged target during exposure, and to a subpopulation of a few highly resistant spores (29). The shoulder seen sometimes on the semilogarithmic survivor curve of strain 33729 (data not shown) was apparently due to heat activation of the dormant spores and therefore was not included in the determinations of rate constants for spore inactivation. The presence of multiple targets makes the accumulation of damage possible, but the rectilinear region on a survival curve still gives the sensitivity of the critical target (27).

The mathematical relations that were used to predict a DSC profile of the critical target in strain 33729 spores are given in the calculations section of Materials and Methods.

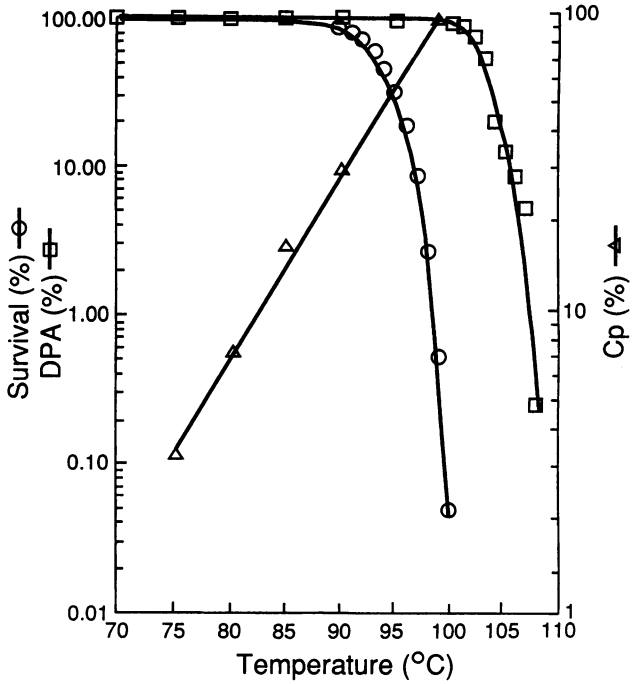

FIG. 7. Semilogarithmic temperature profiles of the survival percentages of dormant native spores calculated from *D*, *z*, and *r* values (○), the DPA release percentages measured directly (□), and the relative specific heat (C_p) taken directly from the exponential part of transition *b* on the DSC profile in Fig. 1A (△).

First, equation 2 was used to calculate the number of spore survivors at specific temperatures in the ascending part of transition *b* (Fig. 1A). At temperatures ranging from 73.5 (T_o) to 100°C (T_m), the number of survivors declined slowly at first (75 to 90°C) and then rapidly (90 to 100°C), as shown in Fig. 7. In the temperature range from 73.5 to 100°C, there was a corresponding exponential rise in the specific heat of the sample. A correlation was thus shown between the calculated loss of spore viability and the observed increase in C_p of transition *b*.

The viability of spores heated in the calorimeter was also determined experimentally. Spore samples, prepared as described above, were heated in the calorimeter to temperatures of 70, 90, 95, 100, and 110°C. After being heated, the sample pans were cooled to 10°C at 200°C/min and opened with sterile pliers. The contents were vortex mixed in 5 ml of nutrient broth for 30 to 60 s. The samples were counted following serial dilution in nutrient broth and plating on Trypticase soy agar. Spore viability values (data not shown) did not differ noticeably from the theoretical values calculated above. The measured rate of spore killing coincided with the ascension in transition *b* shown in Fig. 1A and 6A. Over 99% of the spores were killed between 70 and 100°C, and over 99.9% were killed at 110°C.

Equations 3 and 4 were then used to calculate a predicted DSC transition for target inactivation during killing of the dormant spore population, with both dormant native and dormant decoated spores (Fig. 8). The predicted transitions were insensitive to the low value of T_o (10°C) that was used. The target inactivation rates, with both spore types, were low or zero below 80°C but increased slowly with temperature at first and then more rapidly, to a maximum rate at a temperature denoted by $T_{D_{max}}$ (Table 1), 94.5°C for the native

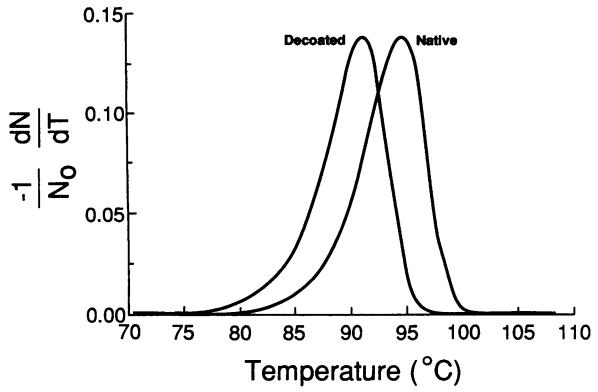

FIG. 8. Critical target inactivation transitions predicted for dormant native spores and dormant decoated spores, on the basis of the heating rate for the DSC scans and calculated from the D and z values in Table 1.

spores and 91.0°C for the decoated spores. The target inactivation rates declined quickly at temperatures beyond $T_{D_{max}}$ and resulted in a single-peaked curve that was somewhat asymmetric. The half-width (ΔT) calculated by equations 5 and 6 was the same for both the native and the decoated spores (Table 1).

No evidence of a peak was observed at $T_{D_{max}}$ in transition b of the actual DSC profiles of the two spore types (Fig. 1A and B). Thus, the magnitude of the transition of the critical target in these profiles must be much smaller than the predicted transition shown in Fig. 8. The values of $T_{D_{max}}$ in the predicted profiles were consistent with known thermal resistance values, although these values may be subject to differences between heating conditions in the calorimeter and those used for determining D and z. These differences were considered inconsequential in the calculations because, at the low scan rate (10°C/min), appreciable thermal gradients were unlikely to be established within the sample. The $T_{D_{max}}$ temperatures were much higher than the minimum temperature of spore killing (about 70°C) because of the relatively rapid scan rate used for DSC, compared with the extremely long exposures required for killing at 70°C (Table 1). Since irreversible inactivation depends on both the temperature and the length of time of exposure, little change would be detectable in a DSC scan of dormant spores even at a scan rate of 10°C/min. At a lower scan rate, however, there would be enough time for denaturation to occur at lower temperatures, and $T_{D_{max}}$ would be lower. The $T_{D_{max}}$ for inactivation of the critical target in dormant native spores, for example, was predicted to be 88.3°C at a scan rate of 1°C/min and 100.7°C at a scan rate of 100°C/min. At each scan rate, the thermosensitivity of the critical target does not change; only the conditions for calculating it are altered. Thus, measurements of $T_{D_{max}}$ are meaningful only when the scan rate is specified. The equations also assume that z does not change as temperature is scanned upward. This may not necessarily hold for all temperatures in the scan, but it does hold for temperatures within the range in which D and z are determined (37). Therefore, the predicted critical target transitions calculated for the native and decoated dormant spores were considered valid.

Release of DPA and A_{240} to A_{280} materials compared with heat killing of spores. Chemical changes that occur during the thermal death of spores can provide useful information about heat killing mechanisms, as exemplified by the findings of El-Bisi et al. (14) and Levinson and Hyatt (29). In particular, the release of intraprotoplast components may indicate disruption of the protoplast membrane and its possible correlation with spore death.

Consequently, the release of the predominant intraprotoplast compound, DPA, was compared with the loss of spore viability in the DSC scan. A graph showing the release of DPA from dormant native spores at specific points during a DSC scan (Fig. 7) indicated a slow initial loss of a small fraction of the DPA (12%) at low temperatures (70 to 100°C) followed by a rapid loss of most of the DPA (88%) at higher temperatures (100 to 108°C), when only 0.05% of the spores remained viable. Spores scanned to higher temperatures quickly lost their remaining DPA, but only after the remaining spores were killed. Thus, the release of most of the DPA occurred after most of the spores had been heat killed. This secondary release of the DPA can be attributed to secondary disruption or permeabilization of the spore protoplast membrane by heat.

The release of cytoplasmic materials absorbing between 240 and 280 nm (proteins and nucleic acids, as well as DPA) was also examined. This release increased with the increase in temperature during the descending part of transition b in the DSC scan, corresponding with the release of DPA and not with the killing of the dormant native spores (data not shown). Most of the released cytoplasmic material absorbed at 270 nm, the absorbance maximum for DPA. The maxima for proteins and nucleic acids at 260 and 280 nm, respectively, were not discernible, although this could have been due to masking caused by the broad peak for DPA spanning 250 to 290 nm.

DISCUSSION

DSC permits intact cells and spores to be analyzed during exposure to increases in temperature. Thermograms of several species of bacterial vegetative cells (2, 9, 26, 30, 31, 37, 46) and spores (32–34, 37) have been published elsewhere, and in general the scans of *B. megaterium* ATCC 33729 spores and cells resemble those of other bacteria with respect to the numbers and positions of the main transitions.

Thermograms of the native dormant spores show only a few transitions, but these can include a larger number of transitions which are not resolvable. The transition in the region of the scans at which loss of viability was observed is irreversible and most probably was due to the unfolding and denaturation of protein. Other macromolecules can contribute to the thermograms, but the irreversible nature of DNA and RNA melting probably constitutes only a minor fraction of the total heat capacity (27). Peak area is a function of the protein concentration and the specific enthalpy of a protein or a group of closely related proteins (2). Thus, large transitions in thermograms of spores and cells will be due either to proteins present at high concentrations or, more likely, to combinations of several proteins with peaks at the same transition temperature. Even with the disadvantage of being unable to determine the contribution of each protein, DSC allows spores to be analyzed concurrently with the measurement of viability. In *B. megaterium* ATCC 33729, the loss of viability of spores heated in the calorimeter was correlated with the second major endotherm, at 100°C (transition b). The first major endotherm, at 56°C (transition a), was correlated with the heat activation of germination, and the third endotherm, at 114°C (transition c), was correlated with the coat-outer membrane complex. Heating spores at

90°C in the calorimeter for different lengths of time indicated that the time course for denaturation of transition *b* closely followed the kinetics for killing of spores.

Our findings by DSC of intact bacterial spores and vegetative cells should be brought into perspective with those of prior investigators. Apparently the earliest such investigation of spores was made in 1974 by Maeda et al. (33), who used freeze-dried dormant and hydration-germinated *B. megaterium* spores. The dried dormant spores showed featureless thermograms. The thermograms of the germinated spores showed endothermic transitions with peaks at 100 and 130°C that seemed to correspond with peaks shown by Ca-DPA. The samples were apparently analyzed in unsealed pans (cf. Maeda et al. [34]), however, so that evaporation of water may have contributed. Thermograms of apparently dormant *B. cereus* spores in the following DSC study by Maeda et al. (34), using sealed pans, showed endothermic transitions with peaks at 56, 95, and 103°C and an exothermic transition with a peak at 105°C, which were roughly comparable to those we observed with dormant native *B. megaterium* spores (if allowance is made for the opposite polarity of plotting). Maeda et al. (34) further demonstrated, by partial scanning to 61°C and by preheating for 1 h at 65°C, that the 56°C transition was attributable to heat activation. This transition was irreversible immediately but reversible after storage for 5 days at room temperature. Our results thus confirm this earlier identification of an activation transition. A further report by Maeda et al. (32) with a more sensitive calorimeter confirmed the previous findings (34) and additionally showed the appearance of a peculiar and unexplained 42°C exothermic peak in the rescan. They further reported that the DSC characteristics associated with heat activation in the intact spores were retained in isolated coats, the protein which they suggested was the site of the activation process. Alternatively, we suggest that a macromolecule (probably a protein) in the protoplast membrane or within the protoplast is more plausible as the site of heat activation, since the DSC activation peak was retained in dormant decoated spores (Fig. 1B).

The only other DSC thermogram of bacterial spores, to our knowledge, is that of dormant *B. cereus* spores by Miles et al. (37). Their findings were roughly comparable to those of Maeda et al. (32, 34), except for the absence of a distinct 56°C transition, which may have been due to the use of stored and thus age-activated spores.

After early descriptive studies (9, 46), DSC of vegetative bacterial cells was systematically studied by Miles et al. (37), who compared the thermograms of eight species having different heat resistances. Major irreversible endotherms at 68 to 73, 77 to 84, 89 to 99, and 105 to 110°C were observed. There was a direct relationship between the onset of thermal denaturation and the thermoresistance values of the different species, and the maximum death rates computed from *D* and *z* values occurred at temperatures above that of the onset of thermal denaturation observed by DSC. A small reversible endotherm with a peak at 90 to 91°C was identified as the melting endotherm of DNA. In a subsequent study, Mackey et al. (31) demonstrated the linear correlation of this peak melting temperature of DNA with the mole fraction of guanine plus cytosine (G+C) in the isolated DNAs of 58 species. Thus, DSC of intact bacterial cells provides a simple method for estimation of their G+C contents without having to isolate and purify the DNA. Recently, Mackey et al. (30) fractionated *Escherichia coli* cells into substituent components (e.g., cell envelopes, cytosol, ribosomes, and their chemical components) and compared the thermogram given by each fraction with that observed in whole cells, thereby identifying most of the 10 main DSC peaks.

Comparative thermal analysis of vegetative bacterial cells was also undertaken by Lepock et al. (26), who used DSC to analyze thermal transitions in two strains of the thermophile *B. stearothermophilus*, the mesophile *B. megaterium*, and the psychrotroph *Bacillus psychrophilus*, their maximum growth temperatures correlating well with the onset of denaturation in the DSC thermograms. Furthermore, these authors developed a concept, based on enthalpy considerations, that the main endothermic transition in the thermograms must be due primarily to the denaturation of a critical protein. Recently, Anderson et al. (2) correlated directly measured cell death of *Listeria monocytogenes* at normal and high NaCl concentrations with the main endothermic transitions obtained by DSC, which they too attributed to protein denaturation and further suggested that ribosomes might be the critical structural locus.

The foregoing body of evidence from DSC studies on bacterial spores and vegetative cells is augmented by another body of evidence from kinetic comparisons for protein denaturation as the cause of thermal death (37a, 39, 42a). The evidence is indirect, relying on the correlation of kinetic and thermodynamic constants (e.g., energy of activation) for the heat denaturation of DNA, RNA, specific enzymes, and representative proteins with the heat killing of bacterial spores (and also of bacterial vegetative cells, eukaryotic cells, and viruses). In all of these biological systems, thermal death essentially represents the inactivation of a single target, governed by pseudo-first-order kinetics and having parameters that correlate with those of proteins but not with those of DNA and RNA. Consideration of target multiplicity negates the likelihood of an enzyme target. Munblit et al. (39) have reviewed, tabulated, and analyzed a literature of 847 references and proposed a unifying hypothesis that a protein subunit in the cytoplasmic membrane is the common critical target in the thermal inactivation of a wide range of organisms, including bacterial spores. It was proposed that the protein subunit becomes denatured and that the membrane therefore becomes dysfunctionally permeabilized, causing death of the cell. (The monograph of Munblit et al. [39] is entirely in Russian, but key portions have been translated into English [18]. Munblit and Trofimov have also published a short related article in English [40]). Early on, Black and Gerhardt (7) demonstrated that the protoplast membrane is disrupted in heat-killed spores, as indicated by the uptake of glucose and a fluorescigenic dye.

These two prior bodies of evidence, taken together with our experimental results, lead us to conclude that the rate-limiting primary target must be a protein, which is denatured irreversibly by heat in a pseudo-first-order reaction that is expressed in a population of spores as a rectilinear exponential thermal-death curve. Spore death coincides with the ascending part of the major irreversible endothermic transition (*b*) in the DSC thermogram.

However, it cannot be that spore death is caused by protoplast hydration and thus heat susceptibility (essentially germination) as the result of disruption of the protoplast membrane, because the heat-killed spores remain refractile and unswollen. Nor can it be that the release of DPA and other cytoplasmic materials causes spore death, because most of their release occurs after most of the spores are killed. Perhaps protein in the protoplast membrane is denatured initially simply because of its peripheral location, followed quickly by the denaturation of a crucial protein within the protoplast, such as in the ribosomes.

ACKNOWLEDGMENTS

This study was supported by contract DAAL03-86-K-0075 and grant DAAL03-90-G-0146 from the Biological Sciences Program of the U.S. Army Research Office.

We thank Gregory Jurzak for technical assistance.

REFERENCES

1. **Ababouch, O., A. Dikra, and F. F. Busta.** 1987. Tailing of survivor curves of clostridial spores heated in edible oils. J. Appl. Bacteriol. **62:**503–511.
2. **Anderson, W. A., N. D. Hedges, M. V. Jones, and M. B. Cole.** 1991. Thermal inactivation of *Listeria monocytogenes* studied by differential scanning calorimetry. J. Gen. Microbiol. **137:** 1419–1424.
3. **Beaman, T. C., H. S. Pankratz, and P. Gerhardt.** 1972. Ultrastructure of the exosporium and underlying inclusions of spores of *Bacillus megaterium* strains. J. Bacteriol. **109:**1198–1209.
4. **Beaman, T. C., H. S. Pankratz, and P. Gerhardt.** 1988. Heat shock affects permeability and resistance of *Bacillus stearothermophilus* spores. Appl. Environ. Microbiol. **54:**2515–2520.
5. **Belliveau, B. H., T. C. Beaman, and P. Gerhardt.** 1990. Heat resistance correlated with DNA content in *Bacillus megaterium* spores. Appl. Environ. Microbiol. **56:**2919–2921.
6. **Bigelow, W. D.** 1921. The logarithmic nature of thermal death time curves. J. Infect. Dis. **29:**528–536.
7. **Black, S. H., and P. Gerhardt.** 1962. Permeability of bacterial spores. III. Permeation relative to germination. J. Bacteriol. **83:**301–308.
8. **Cerf, O.** 1977. Tailing of survival curves of bacterial spores. J. Appl. Bacteriol. **42:**1–19.
9. **Cho, K. C., K. C. Chow, and K. K. Mark.** 1982. A calorimetric study of the thermal transitions of *Halobacterium cutirubrum*. Can. J. Biochem. **60:**419–421.
10. **Chowdry, B. Z., and S. C. Cole.** 1989. Differential scanning calorimetry: applications in biotechnology. Trends Biotechnol. **7:**11–18.
11. **Church, B. D., and H. O. Halvorson.** 1957. Intermediate metabolism of aerobic spores. I. Activation of glucose oxidation in spores of *Bacillus cereus var. terminalis*. J. Bacteriol. **73:**470–476.
12. **De Ley, J.** 1970. Reexamination of the association between melting point, buoyant density and chemical base composition of deoxyribonucleic acid. J. Bacteriol. **101:**738–754.
13. **DiVito, M. P., W. P. Brennan, and R. L. Fyans.** 1986. Thermal analysis: trends in industrial applications. Am. Lab. **18:**83–95.
14. **El-Bisi, H. M., R. V. Lechowich, M. Amaha, and Z. J. Ordal.** 1962. Chemical events during death of bacterial endospores by moist heat. J. Food Sci. **27:**219–231.
15. **Elkind, M. M., and G. F. Whitmore.** 1967. The radiobiology of cultured mammalian cells. Gordon and Breach, New York.
16. **Fitz-James, P. C.** 1971. Formation of protoplasts from resting spores. J. Bacteriol. **105:**1119–1136.
17. **Foster, S. J., and K. Johnstone.** 1990. The trigger mechanism of bacterial spore germination, p. 89–108. *In* I. Smith, R. Slepecky, and P. Setlow (ed.), Regulation of procaryotic development. American Society for Microbiology, Washington, D.C.
18. **Gerhardt, P.** 1991. Thermoinactivation of microorganisms. ASM News **57:**269–270.
19. **Gerhardt, P., and R. E. Marquis.** 1990. Spore thermoresistance mechanisms, p. 17–37. *In* I. Smith, R. Slepecky, and P. Setlow (ed.), Regulation of procaryotic development. American Society for Microbiology, Washington, D.C.
20. **Janssen, F. W., A. J. Lund, and L. E. Anderson.** 1958. Colorimetric assay for dipicolinic acid in bacterial spores. Science **127:**26–27.
21. **Keynan, A., and Z. Evenchik.** 1969. Activation, p. 359–395. *In* G. W. Gould and A. Hurst (ed.), The bacterial spore. Academic Press, Inc., London.
22. **Keynan, A., Z. Evenchik, H. O. Halvorson, and J. W. Hastings.** 1964. Activation of bacterial endospores. J. Bacteriol. **88:**313–318.
23. **Koshikawa, T., T. C. Beaman, H. S. Pankratz, S. Nakashio, T. R. Corner, and P. Gerhardt.** 1984. Resistance, germination, and permeability correlates of *Bacillus megaterium* spores successively divested of integument layers. J. Bacteriol. **159:**624–632.
24. **Lepock, J. R., H. E. Frey, H. Bayne, and J. Markus.** 1989. Relationship of hyperthermia-induced hemolysis of human erythrocytes to the thermal denaturation of membrane proteins. Biochim. Biophys. Acta **980:**191–201.
25. **Lepock, J. R., H. E. Frey, M. P. Heynen, J. Nishio, B. Waters, K. P. Ritchie, and J. Kruuv.** 1990. Increased thermostability of thermotolerant CHL V79 cells as determined by differential scanning calorimetry. J. Cell. Physiol. **142:**628–634.
26. **Lepock, J. R., H. E. Frey, and W. E. Inniss.** 1990. Thermal analysis of bacteria by differential scanning calorimetry: relationship of protein denaturation in situ to maximum growth temperature. Biochim. Biophys. Acta **1055:**19–26.
27. **Lepock, J. R., H. E. Frey, A. M. Rodahl, and J. Kruuv.** 1988. Thermal analysis of CHL V79 cells using differential scanning calorimetry: implications for hyperthermic cell killing and the heat shock response. J. Cell. Physiol. **137:**14–24.
28. **Levinson, H. S., and M. T. Hyatt.** 1969. Heat activation kinetics of *Bacillus megaterium* spores. Biochem. Biophys. Res. Commun. **37:**909–916.
29. **Levinson, H. S., and M. T. Hyatt.** 1971. Distribution and correlation of events during thermal inactivation of *Bacillus megaterium* spores. J. Bacteriol. **108:**111–121.
30. **Mackey, B. M., C. A. Miles, S. E. Parsons, and D. A. Seymour.** 1991. Thermal denaturation of whole cells and cell components of *Escherichia coli* examined by differential scanning calorimetry. J. Gen. Microbiol. **137:**2361–2374.
31. **Mackey, B. M., S. E. Parsons, C. A. Miles, and R. J. Owen.** 1988. The relationship between the base composition of bacterial DNA and its intracellular melting temperature as determined by differential scanning calorimetry. J. Gen. Microbiol. **134:**1185–1195.
32. **Maeda, Y., I. Kagami, and S. Koga.** 1978. Thermal analysis of the spores of *Bacillus cereus* with special reference to heat activation. Can. J. Microbiol. **24:**1331–1334.
33. **Maeda, Y., S. Noguchi, and S. Koga.** 1974. Differential scanning calorimetric study of spontaneous germination of *Bacillus megaterium* spores by water vapor. J. Gen. Appl. Microbiol. **20:**11–19.
34. **Maeda, Y., Y. Teramoto, and S. Koga.** 1975. Calorimetric study on heat activation of *Bacillus cereus* spores. J. Gen. Appl. Microbiol. **21:**119–122.
35. **Marmur, J., and P. Doty.** 1962. Determination of the base composition of deoxyribonucleic acid from its thermal denaturation temperature. J. Mol. Biol. **5:**109–118.
36. **Marquis, R. E., and G. R. Bender.** 1990. Compact structure of cortical peptidoglycans from bacterial spores. Can. J. Microbiol. **36:**426–429.
37. **Miles, C. A., B. M. Mackey, and S. E. Parsons.** 1986. Differential scanning calorimetry of bacteria. J. Gen. Microbiol. **132:**939–952.

37a. **Moats, W. A.** 1971. Kinetics of thermal death of bacteria. J. Bacteriol. **105:**165–171.

38. **Moberly, B. J., F. Shafa, and P. Gerhardt.** 1966. Structural details of anthrax spores during stages of transformation into vegetative cells. J. Bacteriol. **92:**220–228.
39. **Munblit, V. Y., V. L. Talrose, and V. I. Trofimov.** 1985. Thermoinactivation of microorganisms. Science, Moscow. (In Russian.)
40. **Munblit, V. Y., and V. I. Trofimov.** 1985. Compensation effect in the processes of thermal-inactivation of microorganisms. Biophysics **30:**103–109.
41. **Park, J. T., and R. Hancock.** 1960. A fractionation procedure for studies of the synthesis of cell-wall mucopeptide and of other polymers in cells of *Staphylococcus aureus*. J. Gen. Microbiol. **22:**249–258.
42. **Rahn, O.** 1945. Physical methods of sterilization of microorganisms. Bacteriol. Rev. **9:**1–47.

42a. **Rosenberg, B., G. Kemeny, R. C. Switzer, and T. C. Hamilton.** 1971. Quantitative evidence for protein denaturation as the

cause of thermal death. Nature (London) **232:**471–473.
43. **Setlow, P., and A. Kornberg.** 1969. Biochemical studies of bacterial sporulation and germination. XVII. Sulfhydryl and disulfide levels in dormancy and germination. J. Bacteriol. **100:**1155–1160.
44. **Shay, L. K., and J. C. Vary.** 1978. Biochemical studies on glucose initiated germination in *Bacillus megaterium*. Biochim. Biophys. Acta **538:**284–292.
45. **Vary, J. C., J. F. Skomurski, and B. A. Cornell.** 1984. Differential scanning calorimetry of membranes isolated from *Bacillus megaterium* spores. Can. J. Microbiol. **30:**854–856.
46. **Verrips, C. T., and R. H. Kwast.** 1977. Heat resistance of *Citrobacter freundii* in media with various water activities. Eur. J. Appl. Microbiol. **4:**225–231.
47. **White, T. K., J. Y. Kim, and J. E. Wilson.** 1990. Differential scanning calorimetric study of rat brain hexokinase: domain structure and stability. Arch. Biochem. Biophys. **276:**510–517.